AIAA JOURNAL
Vol. 32, No. 1, January 1994

Simple Numerical Criterion for Vortex Breakdown

B. A. Robinson,* R. M. Barnett,* and S. Agrawal†
McDonnell Douglas Corporation, St. Louis, Missouri 63166

Vortex breakdown is currently identified in numerical flow solutions through postprocessing techniques. Although these methods can identify breakdown accurately, they can involve cumbersome data transfer and processing that can be quite time consuming. Therefore, a simple Rossby number criterion is proposed. The criterion is established using solutions to Euler and Navier-Stokes equations for low-speed flow over a flat-plate delta wing at high angles of attack. Comparison with experimental data shows consistent values of Rossby number at breakdown. The proposed Rossby number criterion provides an efficient means of locating breakdown in numerical solutions. It is also straightforward to incorporate in any flow solver.

Introduction

MODERN fighter aircraft are required to maneuver at flight conditions where vortical flow is a dominant feature of the flowfield. At high angles of attack, the vortices can experience a phenomenon called breakdown or burst. The vortex burst phenomenon has been the subject of much study, both experimentally[1,2] and theoretically[3] for more than two decades. A detailed survey of the research conducted in this area is provided in Refs. 2 and 3. The theoretical studies thus far have been of relatively simple cases, such as a vortex confined in a tube or an isolated vortex. Although many researchers have performed experiments to understand the breakdown of both free and confined vortices, there is still no general agreement regarding the essential nature of vortex breakdown, and no reliable breakdown criterion is available for a broad range of geometries and flight conditions.

Great advances in numerical methods and computer architecture in the past decade have made possible the calculation of vortical flows, including breakdown. Several investigators have studied the three-dimensional flows past different geometries at high angles of attack, using both Euler and Navier-Stokes equations. A widely studied configuration is the flat-plate delta wing with sharp leading edges.[4–8]

Reliable prediction of vortex breakdown depends on how accurately the flowfield is obtained experimentally or analytically. Experimental investigations have made use of different flow visualization techniques to determine the location of vortex breakdown. Smoke particles and various lighting arrangements, including laser light sheets and Schlieren systems, have been employed.[9–11] The exact breakdown position selected by the experimentalists varies according to the criteria each has adopted to select the point of vortex breakdown. In general, these differences in criteria result in a relative difference in breakdown location of at most on the order of the vortex core diameter.

Figure 1 shows one criterion used to visually determine the vortex breakdown position. Upstream of breakdown, the vortex core appears as a smoke-free, dark-colored region at the center of the vortex. The tight vortex has spun smoke particles out of the region, so it appears dark. At the onset of vortex breakdown, the dark core region disappears as smoke enters this area for the first time. The disappearance of the smoke-free core region at breakdown is due to flow stagnation and mixing at the core. With a scanning laser light sheet, the relative accuracy and repeatability of this method are quite good, being limited by the unsteadiness of the vortex breakdown location. For the 70 deg delta wing, the burst was observed to oscillate over a range of approximately 3% of root chord.[9]

Other approaches to breakdown determination from numerical flow solutions have been based on the collapse of the rolled-up shear layer and the stagnation or asymmetry of axial velocity contours.[4,7] In addition, particle traces generated by graphics programs such as PLOT3D[12] can provide indications of breakdown similar to experimental flow visualization. Care must be taken to introduce a sufficient number of particles at appropriate locations to clearly show the onset of breakdown. One difficulty with these approaches is that the relative unsteadiness of the breakdown position cannot be observed without examining the flowfield at several different iterations in the solution. Moreover, these methods require the flowfield data to be reduced external to the flow solver and viewed graphically. Misinterpretation of these analyses may result if, for example, one does not examine the particle traces near the vortex center. Adaptation of these visual techniques to numerical solutions is difficult and not amenable to automation.

Therefore, a simple criterion based on Rossby number, a local nondimensional parameter, is proposed here. Although such an approach has been advanced by several researchers in the past,[11,13–16] an explicit treatment of delta wings in low-speed flow using numerical solutions and experimental data to substantiate the Rossby number criterion has not been available.

The purpose of this study is to compare several different methods of locating the burst point with experimental data and then to develop a simple Rossby number criterion that can be effectively used in the prediction of vortex breakdown. Euler and Navier-Stokes (laminar and turbulent) solutions are analyzed on a flat-plate delta wing with a 70 deg leading-edge sweep and 25 deg bevel on the lower surface along the leading and trailing edges, as shown in Fig. 2. An extensive experimental database also exists for this configuration.[10]

Grid Topology

An H-O type of grid topology for a half-plane model of the delta wing was used in this study; only symmetric flows about the centerline were considered. The grid dimensions are 61 (axial), 65 (radial), and 89 (circumferential). There are 41 points along the wing in the chordwise direction. The surface grid, symmetry plane, and crossflow plane are shown in Fig. 3.

The grid was constructed by successive generation of two-dimensional grids normal to the wing centerline. They were generated using a computer program that solves an elliptic system of partial differential equations.[17] This procedure results in a high-quality orthogonal grid, including difficult areas such as the sharp leading edge of the wing.

Numerical Method

The CFL3D Euler/Navier-Stokes code[18] was used to calculate all of the flowfields in this study. The computational algorithm is

Presented as Paper 92-0057 at the AIAA 30th Aerospace Sciences Meeting, Reno, NV, Jan. 6–9, 1992; received Jan. 30, 1992; revision received March 11, 1993; accepted for publication March 11, 1993.

*Senior Engineer, Aerodynamics. Member AIAA.
†Technical Specialist, Aerodynamics. Associate Fellow AIAA.

based on a thin-layer approximation to the three-dimensional, time-dependent, conservation law form of the compressible Navier-Stokes equations. The code solves the discretized flow equations implicitly using an upwind-biased spatial differencing scheme with either flux difference splitting or flux vector splitting for the convective and pressure terms, and central differencing for the shear-stress and heat-transfer terms. In this study, the Roe-averaged flux difference splitting was applied for the spatial terms. Flux limiting was also used to alleviate oscillations near high gradient flow regions. The effect of turbulence in the flowfield calculations was obtained using the standard Baldwin-Lomax model.

Breakdown Criteria

Different criteria for determining vortex breakdown locations exist in the literature. For example, particle traces can give a qualitative picture of the flowfields in the leading-edge vortex. The abrupt change in the traces from a regular, ordered structure is an indication of the vortex breakdown occurring in the flowfield. This is illustrated in Fig. 4. The breakdown locations are identified by inspection of the streamwise component of velocity on each axial grid plane using PLOT3D. A rapid decrease in this velocity component and increase in vortex core size are observed at the onset of vortex breakdown. Although the particle traces give a reasonably good idea of the breakdown location, they are still very qualitative.

The apparent collapse of the rolled-up vortex sheet or shear layer provides another method of identifying vortex breakdown.[4] This sheet can be traced by plotting the locus of maximum swirl angle (helical angle) in an axial plane by performing radial surveys

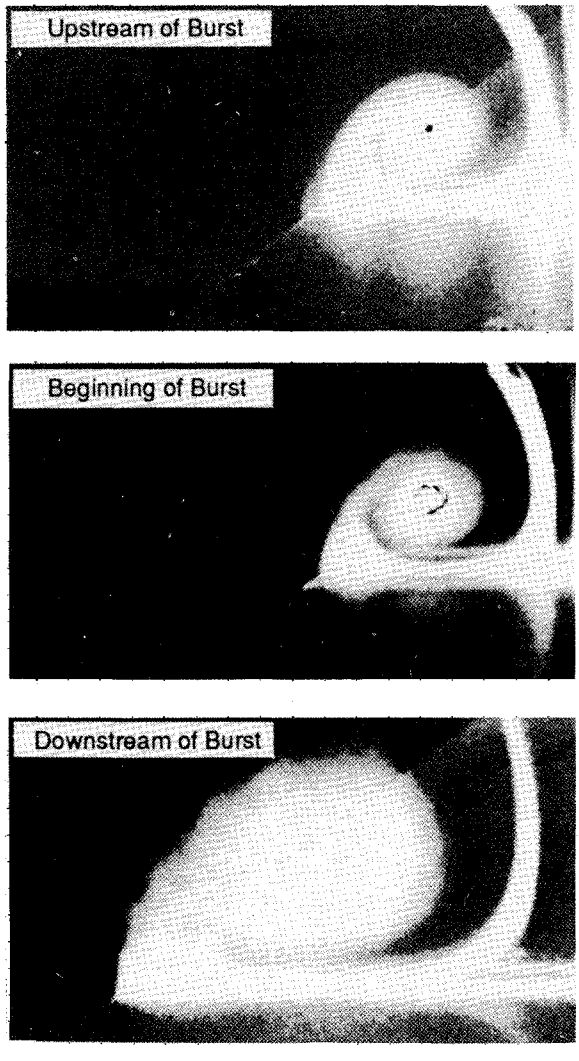

Fig. 1 Detection of vortex breakdown using a laser sheet (Ref. 9).

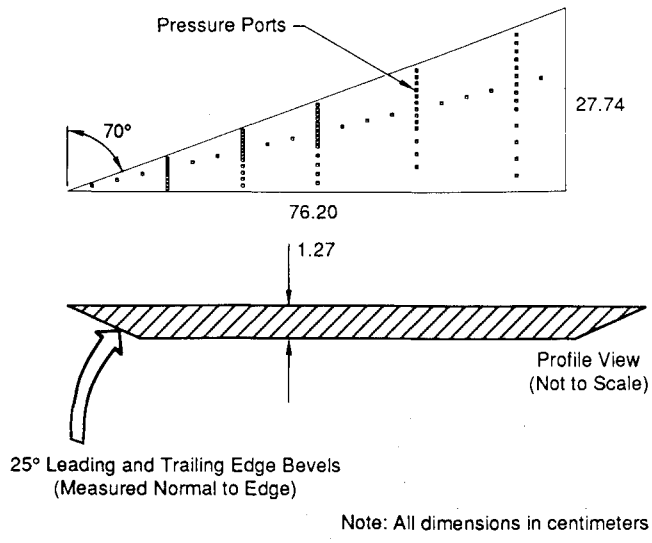

Fig. 2 Flat-plate semispan delta wing model.

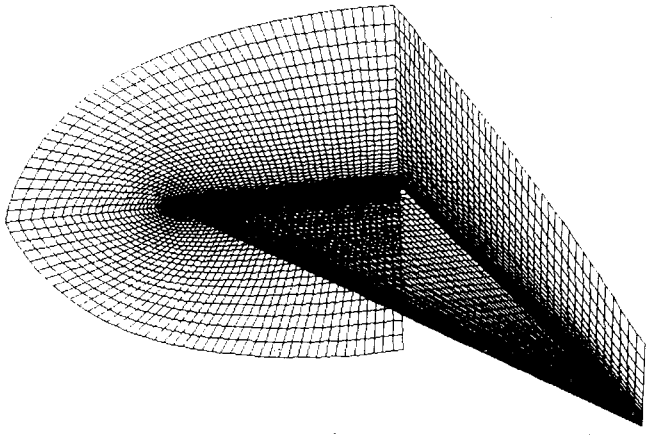

Fig. 3 Partial view of the delta wing grid: 61 (axial) × 65 (radial) × 89 (circumferential).

outward from the vortex center. At each plane, the center of the vortex is determined by locating the point of minimum total pressure, and the loci are examined for every streamwise station until the partial or full collapse of these loci onto the vortex center is observed. At the onset of breakdown, a rapid disintegration of the well-defined vortex structure into a diffuse, vortical wakelike flow structure takes place. Figures 5a–5d show shear layer plots at four stations: well ahead of breakdown, just upstream of breakdown, at the onset of breakdown, and downstream of breakdown. It is clearly illustrated that the shear layer, defined in this manner, stays intact until the flow reaches the station located at $x/c = 0.525$, where collapse is observed, indicating breakdown. This collapse is due to flow stagnation in the core region causing the radial surveys for maximum swirl angle to become ineffective.

A more refined criterion for the onset of breakdown is based on the axial velocity distribution in the primary vortex.[2,7] To accomplish this, the flow velocities are transformed to a vortex-based coordinate system, and the axial velocities are examined using contour plots. Figures 6a–6d show axial velocity contours at about the same stations as illustrated in Figs. 5a–5d. Note that ahead of breakdown, the contours have a symmetric structure with the maximum axial velocity residing in the well-defined core of the vortex (Fig. 6a). At axial stations further downstream, however, the core becomes more diffuse (Fig. 6b) and, eventually, the contours show an asymmetric structure and the core becomes ill-defined (Figs. 6c–6d). The burst point is thus determined by locating the axial station where this asymmetry in the axial velocities or stagnation

at the core relative to the edge of the vortex is first observed. This method is consistent with experimental observations and also shear-layer collapse analysis.

Although the criteria just outlined for locating the vortex breakdown are fairly accurate, the task of extracting the breakdown location may require several hours of postprocessing time. For more rapid engineering analysis, therefore, a Rossby number criterion is proposed. The Rossby number Ro is a ratio of the axial and circumferential momentum in a vortex.[19] A standard definition of Ro is

$$Ro = \frac{U}{r\Omega}$$

where U is a core axial velocity, ω is a rotation rate, and r is an effective radius of the vortex. The determination of these three quantities is restricted only in that they should be representative of the vortex and, therefore, do not restrict the proposed breakdown criterion to either bubble or spiral type. For a mathematical model, these values may be determined analytically, but a more typical approach for experimental and numerical solutions is to use an integral method to calculate these quantities. In this study, an integral-based approach is used, in which the axial velocity and rotation rate are integrated over the primary vortical region, the area of which defines an effective radius. A similar approach has been applied to experimental data with good success.[11]

Implementation of this method is straightforward. The velocities are first transformed into the vortex-axis system and then are normalized by the freestream velocity. Distances are nondimensionalized by the root chord. A nondimensional vorticity ω is then calculated for each cell using Stokes' theorem. The area A, consisting of the vortical flow on the lee side of the wing exhibiting the same sign in vorticity as the primary vortex, is defined by the cells that have $\omega \geq 1$. This value was chosen by observing the areas resulting from several different values of ω. Figure 7 shows an example of the area A defined by $\omega \geq 1$.

The circulation Γ can be obtained by integrating the vorticities over this area as

$$\Gamma = \Sigma\, \omega\, dA$$

The rotation rate and effective radius are then calculated as

$$\Omega = \frac{\Gamma}{2A}, \qquad r = \sqrt{\frac{A}{\pi}}$$

Finally, the axial velocity is calculated by integrating the velocity component v' along the vortex axis, over an area defining the vortex core A'.

$$U = \frac{\Sigma v'\, dA'}{\Sigma\, dA'}$$

The area A' is defined by a circle centered at the centroid of vorticity ($\omega \geq 1$) with some small radius consistent with the size of the vortex. For this study, a radius of 20% of the distance from the centroid of vorticity to the surface of the wing was used. The value of 20% was chosen because it results in a fairly small area near the core, yet an area large enough to accommodate the flow resolution.

This approach is similar to that used by Cornelius,[11] where the rotation rate and radius are integrated quantities. By using an integrated axial velocity, the Rossby number behaves smoothly in both the pre- and postbreakdown regions.

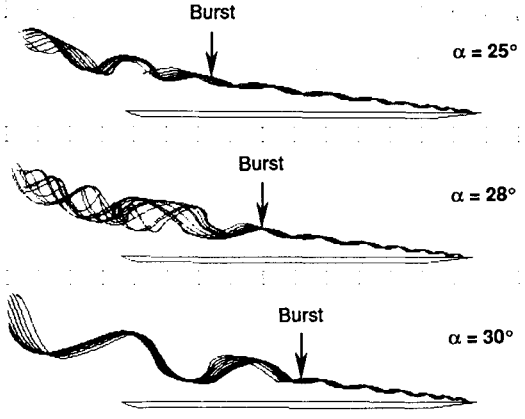

Fig. 4 Vortex breakdown indicated with particle traces: $M_\infty = 0.30$, $Re_c = 1 \times 10^6$, laminar solution.

Results

Flowfields calculated using the CFL3D code were analyzed to determine the location of vortex breakdown for the delta wing. The

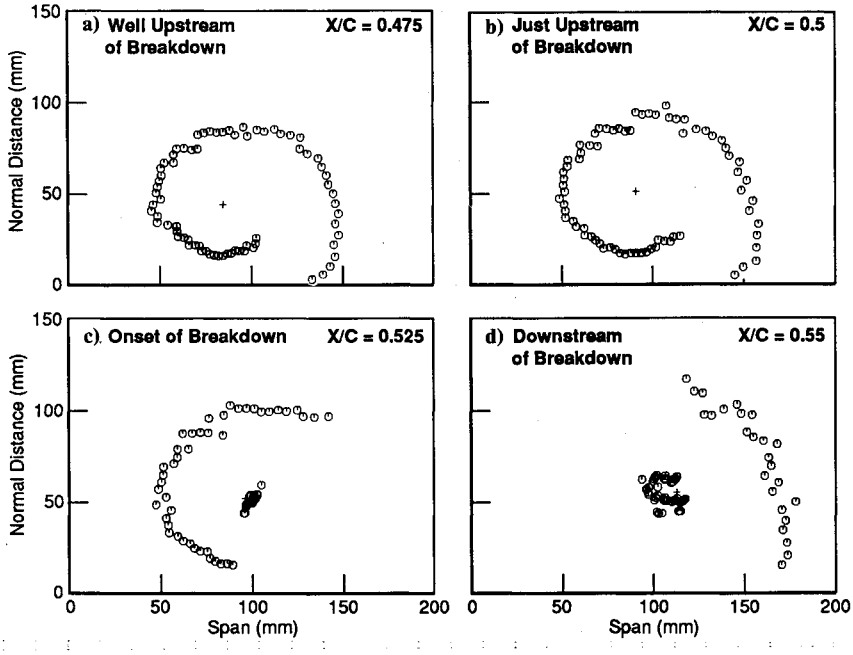

Fig. 5 Identifying vortex breakdown from shear-layer collapse: $M_\infty = 0.30$, $\alpha = 30$ deg, $Re_c = 1 \times 10^6$, laminar solution.

results were obtained for a freestream Mach number M_∞ of 0.3 at several angles of attack α. Most of the analyses were performed at $\alpha = 30$ deg. The Reynolds number based on the root chord for these calculations was 1.0×10^6. In general, the residuals dropped two to three orders of magnitude and the integrated forces converged to a nominal value with a 2% oscillation.

Figures 5 and 6 show breakdown identification using two different criteria: the collapse of the shear layer and the stagnation/asymmetry of the axial velocity contours. For the case shown, these two criteria agree to within 2.5% of the root chord or one cell width, with Fig. 5 showing breakdown at $x/c = 0.50$ and Fig. 6 breakdown at $x/c = 0.525$. The basis behind these two criteria is the stagnation of axial flow in the core of the vortex at breakdown due to a large adverse pressure gradient. Figure 8a illustrates the axial pressure (nondimensionalized by freestream density and speed of sound) in the core for the same flow conditions shown in Figs. 5 and 6. The axial pressure gradient is depicted in Fig. 8b. It is apparent from this figure that breakdown occurs just downstream of the maximum adverse pressure gradient along the core.

Although these two approaches yield consistent breakdown locations, the methods are quite cumbersome, requiring postprocessing and a plane-by-plane graphical analysis. The same breakdown location information can be obtained as the flow solver is running by using the Rossby number criterion proposed here.

The Rossby number calculation described earlier has been implemented into the CFL3D code. A typical example of how the quantities U, r, and ω vary along the chord for a vortex shed from a sharp leading-edge delta wing at high angle of attack is shown in Fig. 9. These plots are for a laminar solution for $M_\infty = 0.3$ and $\alpha = 30$ deg. The core axial velocity reaches a peak at about 10% of the root chord as the flow experiences a favorable pressure gradient (Fig. 9a). This core velocity then decreases slowly until the flow reaches 45% of the root chord, where there is a rapid decrease due to the strong adverse pressure gradient near vortex breakdown. Beyond this point, the vortex is burst and the location of the vortex core becomes somewhat vague. Complete stagnation of the core axial velocity does not always appear near breakdown in this numerical analysis due to the area-weighted integration employed to calculate this quantity. The effective core radius is shown in Fig. 9b. This quantity increases steadily along the chord. There is a discontinuity at about 50% of the root chord near breakdown due to the sudden expansion of the vortex. The rotation rate, similar to the core axial velocity, reaches a maximum at about 10% of the root chord and then decreases steadily along the chord as shown in Fig. 9c. Again, there is a discontinuity at about 50% of the root chord, near the burst location, due to the rapid expansion of the vortex.

A plot of Rossby number variation along the chord is depicted in Fig. 10. Ro is found to have a maximum close to the apex of the delta wing and then decreases along the chord. A sharp decrease at about 50% of the root chord is driven by the decrease in axial core velocity shown in Fig. 9a. This decrease occurs in the region of breakdown predicted by the shear-layer collapse shown in Fig. 5c and the asymmetric axial velocity contours illustrated in Fig. 6c.

Changing the limit on ω to define A and the limit on the core radius to define A' will change the values used in the Rossby number calculation. Decreasing the limit on ω to values less than 1 will result in a larger (more diffuse) area of integration possibly extending into regions well outside the primary vortex. Increasing the limit on ω restricts the area of integration to smaller and smaller areas around the vortex core. Increasing the limit on the core radius will result in an integration over a larger portion of the vortex. This will effectively smooth the axial velocity distribution shown in Fig. 9a and result in a smaller gradient near burst. Decreasing

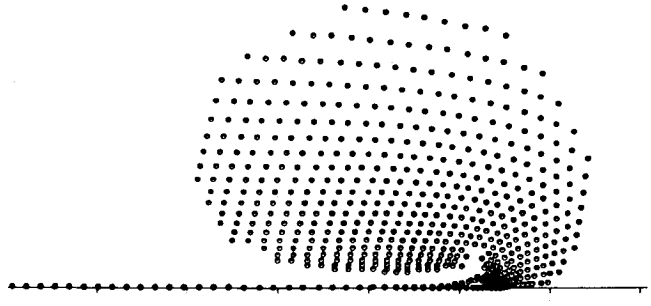

Fig. 7 Example of integration area defined by $\omega \geq 1$.

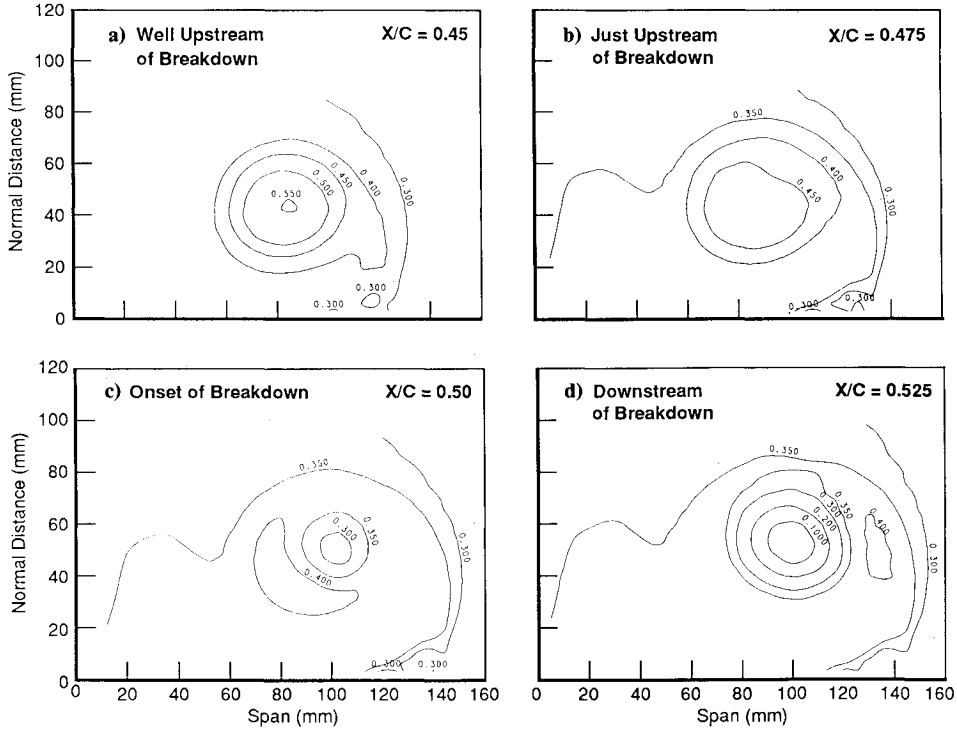

Fig. 6 Identifying vortex breakdown from axial velocity contours: $M_\infty = 0.30$, $Re_c = 1 \times 10^6$, laminar solution.

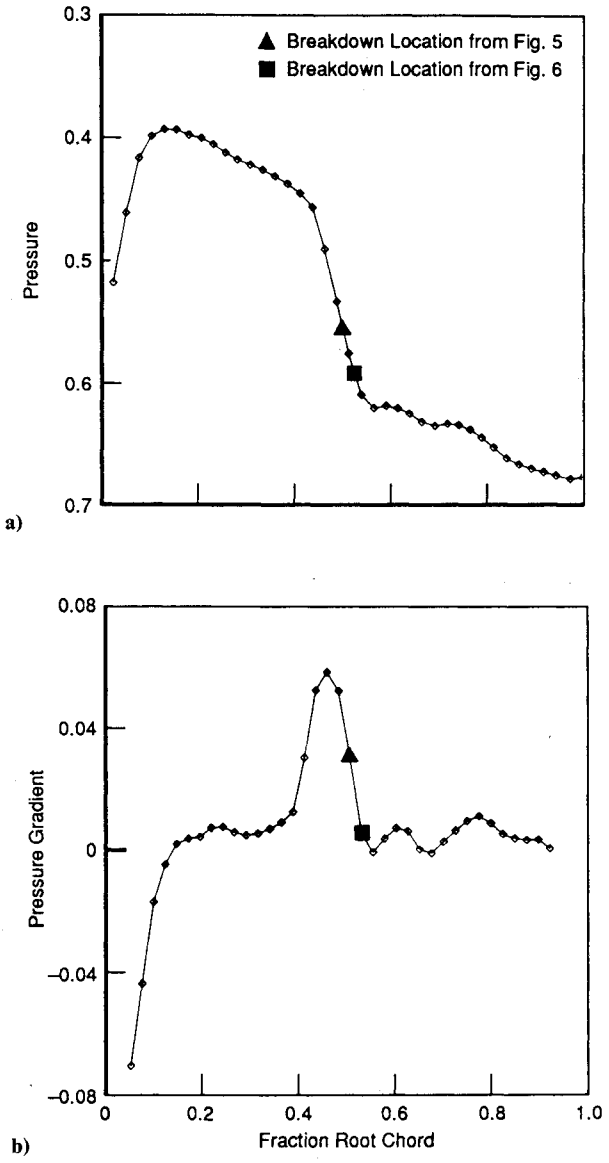

Fig. 8 Pressure variation along the vortex core: $M_\infty = 0.30$, $\alpha = 30$ deg, $Re_c = 1 \times 10^6$, laminar solution.

the limit on the core radius is desirable; however, it must not be decreased to the point that the grid resolution compromises the integration.

Ro variation along the chord for several angles of attack is shown in Fig. 11 from Euler, laminar, and turbulent calculations. This figure shows that Rossby numbers corresponding to burst locations fall in a narrow band from 0.9 to 1.4. Another important feature to notice in Fig. 11 is that the $\alpha = 20$ deg case, which does not experience breakdown, shows no sharp decrease in *Ro*. It is also interesting to note that the variations in *Ro* with angle of attack are small in the prebreakdown regions (except near the apex), whereas near the onset of breakdown, such variations are large. In the postbreakdown regions, *Ro* is usually small (below 1.0). These results, therefore, clearly indicate a narrow band of Rossby number (0.9 to 1.4), above which the vortex remains stable. Below a value of 0.9, the vortex will be burst. Slight changes to the limits on ω and the core radius result in similar Rossby number behavior along the chord with the same narrow band of critical values at breakdown. It should be noted that, in general, fluctuations in *Ro* are observed as the solution converges. It has been shown that for α less than approximately 30 deg, the Rossby number remains fairly constant at a given chordwise station. At higher angles of attack, however, the Rossby number fluctuates downstream of the burst location, indicating unsteadiness in the flow.[20]

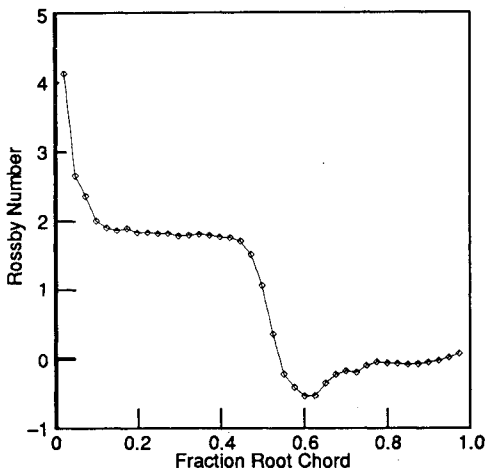

Fig. 10 Example of Rossby number variation along the chord, laminar solution: $M_\infty = 0.30$, $\alpha = 30$ deg, $Re_c = 1 \times 10^6$.

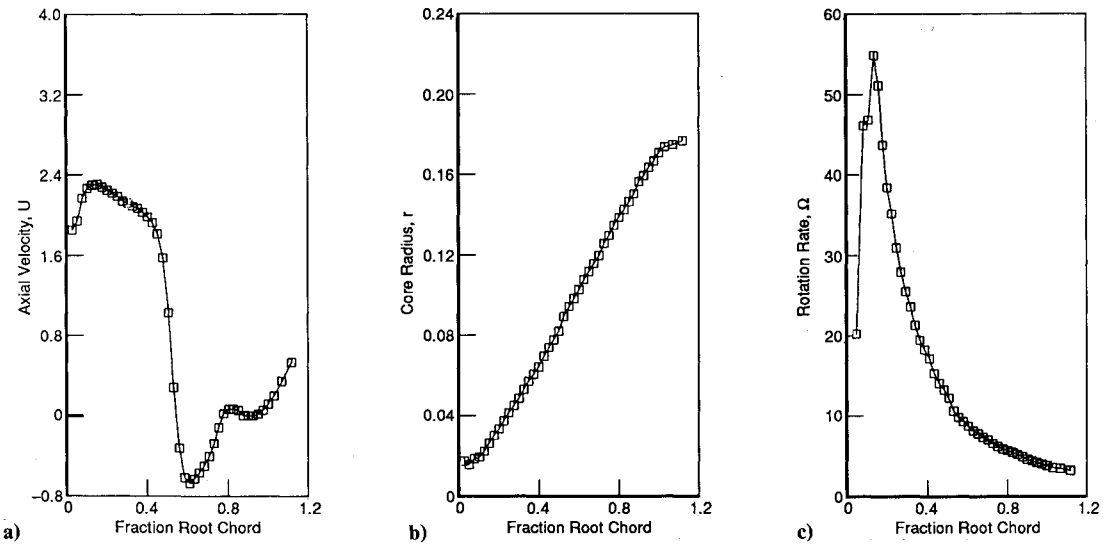

Fig. 9 Variables used in Rossby number calculations: $M_\infty = 0.30$, $\alpha = 30$ deg, $Re_c = 1 \times 10^6$, laminar solution.

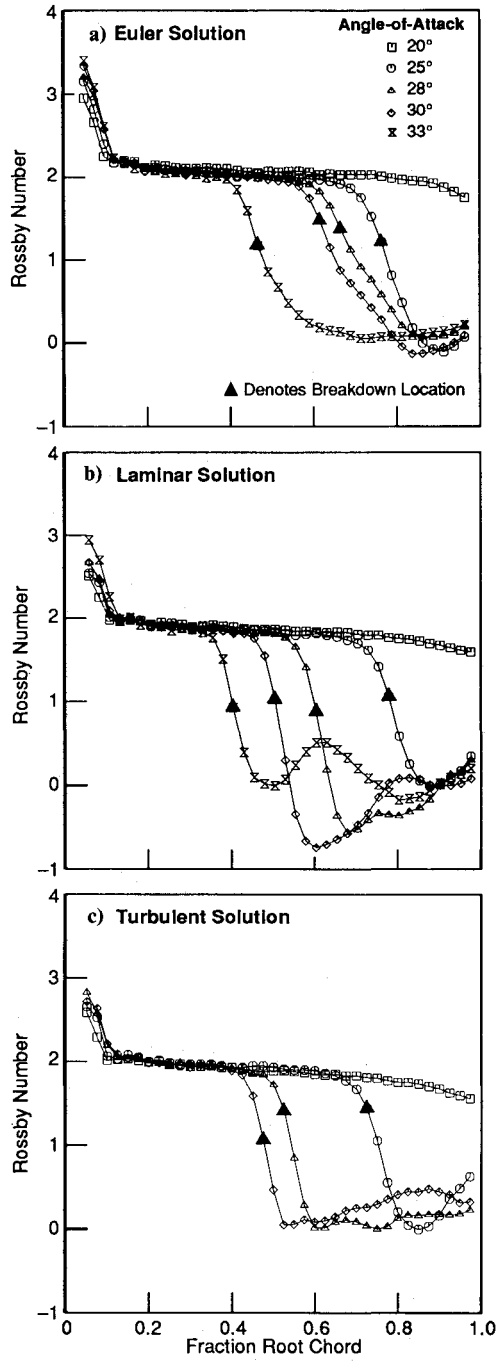

Fig. 11 Effect of angle of attack on Rossby number: $M_\infty = 0.30$, $\alpha = 30$ deg, $Re_c = 1 \times 10^6$.

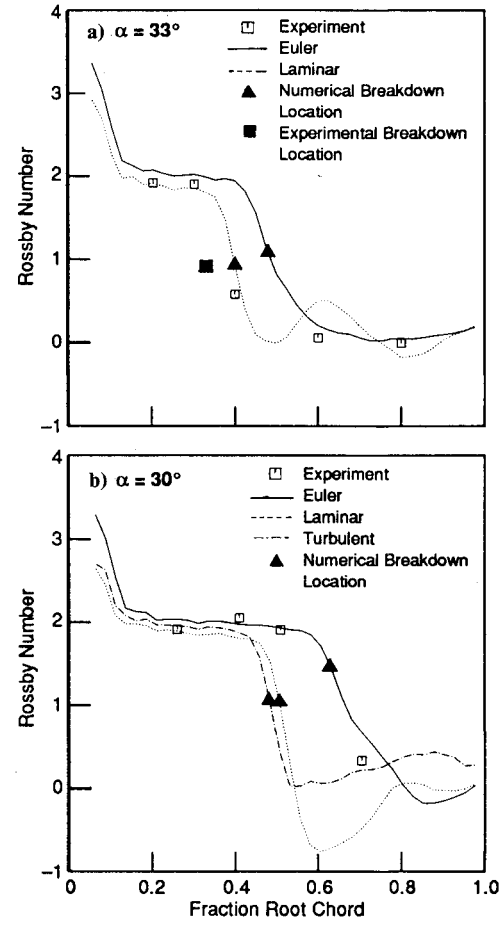

Fig. 12 Rossby number comparison with experiments: $M_\infty = 0.30$, $Re_c = 1 \times 10^6$.

Experimental data also were analyzed in the same manner as the computational results. Three-dimensional velocity fields on a 70-deg delta wing were measured using LDV (laser Doppler velocimetry), which resulted in arrays of flow velocity data defined at discrete locations on two-dimensional planes through the vortex.[9] The procedures to provide *Ro* data for the numerical flow solutions were applied to the experimental flowfields using the same nondimensionalizations and vorticity integration limits. A comparison of experimental and numerical *Ro* variation along the chord is shown in Fig. 12. Euler and laminar data along with the experiment are illustrated in Fig. 12a for $\alpha = 33$ deg. Rossby numbers corresponding to the pre- and postbreakdown regions are in fair agreement with test data. Rossby numbers at breakdown are 1.1 and 0.9 for the Euler and laminar flows, respectively. Experiment showed burst at $x/c = 0.33$, corresponding to $Ro \simeq 1.0$. Euler, laminar, and turbulent results are shown with test data for $\alpha = 30$ deg in Fig. 12b. Again, a comparison of pre- and postbreakdown Rossby numbers indicates fair agreement between experiment and computation. The numerical data show that the Rossby number at breakdown lies between 1.0 and 1.4. The experimental data are sparse in the region, $x/c = 0.58$, for this case. The experimental *Ro* upstream of breakdown is 1.9 and downstream of breakdown it is 0.4. The test data shown in Fig. 12, as well as the limited experimental data pertaining to leading-edge vortex breakdown presented in Ref. 13, suggest a critical value of approximately 1.0 for such flows. Further correlation studies are needed to establish the validity of these critical values of *Ro* on other types of geometries and for other flow conditions.

Conclusions

A vortex breakdown criterion based on an integral formulation of the Rossby number is proposed. The criterion for a vortex shed from a sharp leading-edged, highly swept delta wing in low-speed flow has been established using solutions to the Euler and Navier-Stokes equations. Breakdown locations identified by more established criteria have been correlated with Rossby number variation along the chord. The critical Rossby number found in this study falls in a range of 0.9 to 1.4. Values below this range indicate a burst vortex, whereas those above this range suggest a stable vortex. Comparisons with experimental results show similar values of Rossby number at breakdown, as well as in the pre- and postbreakdown regions.

The Rossby number provides a quantitative approach to determining the state of a vortex, i.e., burst or unburst. This technique can improve the efficiency of locating vortex breakdown within a flow solution as it eliminates the need for cumbersome postprocessing. This numerical criterion is straightforward and can be used with any flow solver.

Acknowledgments

This study was supported by the McDonnell Douglas Independent Research and Development program. Computer resources for this work were provided by the Numerical Aerodynamic Simulation facility as part of a study sponsored by Terry Holst of the NASA Ames Research Center. The authors also express their appreciation to Alan Cain of McDonnell Douglas Aerospace for fruitful discussions. Experimental data were obtained by McDonnell Douglas Aerospace as part of a U.S. Navy-funded investigation of leading-edge vortex behavior on delta wings.

References

[1]Lambourne, N. C., and Bryer, D. W., "The Bursting of Leading-Edge Vortices—Some Observations and Discussion of the Phenomenon," Aeronautical Research Council, Reports & Memoranda No. 3282, April 1961.

[2]Escudier, M., "Vortex Breakdown: Observations and Explanations," *Progress in Aerospace Sciences*, Vol. 25, No. 2, 1988, pp. 189–229.

[3]Leibovich, S., "Vortex Stability and Breakdown: Survey and Extension," *AIAA Journal*, Vol. 22, No. 9, 1984, pp. 1192–1206.

[4]O'Neil, P. J., Barnett, R. M., and Louie, C. M., "Numerical Simulation of Leading-Edge Vortex Breakdown Using an Euler Code," *Journal of Aircraft*, Vol. 29, No. 3, 1992, pp. 301–307.

[5]Hartwich, P. M., Hsu, C. H., Luckring, J. M., and Liu, C. H., "Numerical Study of the Vortex Burst Phenomenon for Delta Wings," AIAA Paper 88-0505, Jan. 1988.

[6]Ekaterinaris, J. A., and Schiff, L. B., "Vortical Flows over Delta Wings and Numerical Prediction of Vortex Breakdown," AIAA Paper 90-0102, Jan. 1990.

[7]Agrawal, S., Barnett, R. M., and Robinson, B. A., "Numerical Investigation of Vortex Breakdown on a Delta Wing," *AIAA Joumal*, Vol. 30, No. 3, 1992, pp. 584–591.

[8]Robinson, B., Barnett, R., and Agrawal, S., "A Simple Numerical Criterion for Vortex Breakdown," AIAA Paper 92-0057, Jan. 1992.

[9]O'Neil, P. J., Roos, F. W., Kegelman, J. T., Barnett, R. M., and Hawk, J. D., "Investigation of Flow Characteristics of a Developed Vortex," Final Rept., Naval Air Development Center, NADC-89114-60, May 1989.

[10]Wentz, W. H., and Kohlman, P. L., "Wind Tunnel Investigations of Vortex Breakdown on Slender Sharp-Edged Wings," NASA Res. Grant NGR-17-002-043, Final Rept., Nov. 1968.

[11]Cornelius, K. C., "3-D Analysis of Laser Measurements of Vortex Bursting On a Chined Forebody Fighter Configuration," AIAA Paper 90-3020, Aug. 1990.

[12]Buning, G. P., and Steger, J. L., "Graphics and Flow Visualization in Computational Fluid Dynamics," AIAA Paper 85-1507, July 1985.

[13]Wilson, J. D., "Calculation of Vortex Breakdown Locations for Flow over Delta Wings," *Journal of Aircraft*, Vol. 14, No. 4, 1977, pp. 1020–1022.

[14]Spall, R. E., Gatski, T. B., and Grosch, C. E., "A Criterion For Vortex Breakdown," *Physics of Fluids*, Vol. 30, Nov. 1987, pp. 3434–3440.

[15]Spall, R., and Gatski, T., "A Computational Study of the Taxonomy of Vortex Breakdown," AIAA Paper 90-1624, June 1990.

[16]Le, T. H., Mege, P., and Morchoisne, Y., "Determination de Criteres d'Eclatement Tourbillonnaire par Resolution des Equations d'Euler et de Navier Stokes," *AGARD-FDP Symposium on Vortex Flow Aerodynamics*, Paper No. 2, Oct. 1990.

[17]Thomson, J. F., Thames, F. C., and Mastin, C. W., "Automatic Numerical Generation of Body-Fitted Curvilinear Coordinate System for Field Containing Any Number of Arbitrary Two-Dimensional Bodies," *Journal of Computational Physics*, Vol. 15, No. 3, 1974, pp. 299–319.

[18]Thomas, J. L., Taylor, S. L., and Anderson, W. K., "Navier-Stokes Computations of Vortical Flows over Low Aspect Ratio Wings," AIAA Paper 87-0207, Jan. 1987.

[19]Bachelor, G. K., *An Introduction to Fluid Dynamics*, Cambridge Univ. Press, Cambridge, England, UK, 1967, pp. 555–559.

[20]Agrawal, S., Robinson, B., and Barnett, R., "Prediction of Vortex Breakdown on a Delta Wing," Fifth Symposium on Numerical and Physical Aspects of Aerodynamic Flows, Long Beach, CA, Jan. 1992.